Traffic 2007; **8:** 1035–1051
Blackwell Munksgaard

doi: 10.1111/j.1600-0854.2007.00582.x

Differential Requirements for ts-O45-G and Procollagen Biosynthetic Transport

Vytaute Starkuviene and Rainer Pepperkok

Cell Biology and Cell Biophysics Unit, European Molecular Biology Laboratory, 69117 Heidelberg, Germany
Corresponding authors: Vytaute Starkuviene, starkuvi@embl-heidelberg.de and Rainer Pepperkok, pepperko@embl-heidelberg.de

Emerging experimental evidence favours the existence of cargo sorting occurring upon the endoplasmic reticulum (ER) exit. Recent studies revealed that, in contrast to the conventional secretory marker ts-O45-G, procollagen (PC I) exits the ER at sites not coated with coat protein II and is transported to the Golgi complex in carriers devoid of coat protein I. Here, we investigated whether PC I trafficking requires a different molecular machinery in comparison with the ts-O45-G. By combining colocalization of the cargoes with endogenous markers, downregulation of transport machinery by RNA interference and knock-ins by complementary DNA over-expression, we provide strong evidence that PC I and ts-O45-G have common but also different molecular requirements during pre- and post-Golgi trafficking events.

Key words: cargo sorting, COPI, ER to Golgi transport, Hsp47, procollagen

Received 5 September 2006, revised and accepted for publication 10 April 2007, uncorrected manuscript published online 12 April 2007, published online 5 June 2007

In eukaryotic cells membrane, traffic between the endoplasmic reticulum (ER) and the Golgi complex involves the vesicular coat complexes coat protein II (COPII) and COPI. The COPII mediates cargo concentration of secretory cargo into COPII-coated vesicles and coat protein (COPI)-coated carriers recycle material from post-ER membranes back to the ER (reviewed in 1).

In contrast to this simple transport model, which has been clearly demonstrated for several model transport proteins in yeast and higher eukaryotes, a complexity of cargo sorting at the ER–Golgi boundary with respect to different secretory cargo is becoming increasingly evident. Different yeast secretory proteins show a differential sensitivity in their secretion efficiency in COPI mutant strains (2). The COPII-coated vesicles containing glycosyl-phosphatidylinositol-anchored proteins could be shown to be distinct from ER-derived COPII-coated vesicles transporting amino acid permease Gap1p, alkaline phosphatase and glycosylated pro α factor (3). In mammalian cells, the cystic fibrosis transmembrane conductance regulator (CFTR) transits to the Golgi complex in a 'non-conventional' manner, which does not depend on the activities of ADP ribosylation factor 1 (ARF1), Rab1, Syn5 (4), all three are factors that have been demonstrated to be involved in ER to Golgi transport of conventional transport markers (5–7). Interestingly, trafficking of potassium channel interacting proteins and potassium channel proteins are completely abrogated if the COPI machinery is perturbed, but surprisingly, it is not sensitive to the impairment of COPII function (8). Despite these evidences for the existence of different trafficking routes for different secretory cargo in ER to Golgi transport, a molecular description of these cargo-specific ER exit pathways remains elusive. A secretory cargo molecule of particular interest in this context is procollagen (PC I), which forms a rod-like structure of more than 300 nm in size (for review, see 9). Because of this size, PC I should not be able to enter small 60–80 nm COPII-coated vesicles, which are known to carry conventional secretory cargo out of the ER (10–11). The question how PC I exits the ER is therefore a challenging problem whose study should help to understand the molecular mechanisms underlying differential sorting of specialized secretory cargo at the ER. Interestingly, using a green fluorescent protein (GFP)-tagged version of PC I, it has been proposed that PC I is transported from the ER to the Golgi complex in carriers distinct from those that carry the transport model protein ts-O45-G or endogenous proteins such as ER–Golgi intermediate compartment 53 (ERGIC53) (12). In support of these data, ultrastructural analyses by electron microscopy have shown that PC I is concentrated and leaves the ER at sites devoid of COPII (13). However, in contrast to this, it has also been demonstrated that expression of a GTP-restricted, dominant-negative Sar1p mutant [SAR1p$^{[H79G]}$; (14)], which locks the COPII coat on membranes, is required for the ER exit of PC I (15).

In the present study, we have addressed the hypothesis that the above described differences in ER to Golgi trafficking of PC I, compared with that of conventional cargo, would necessitate at least partially distinct molecular transport machinery. To this end, we exploited fluorescent microscope-based functional assays in intact cells, which previously identified 20 new proteins that affected the trafficking of ts-O45-G when over-expressed (16). Our data show that several of the molecules affecting ts-O45-G transport when over-expressed do not affect PC I trafficking and vice versus. Ts-O45-G and PC I were differently affected by RNA interference (RNAi) downregulation of several well-characterized proteins of the early secretory pathway. In addition, quantitative colocalization studies

demonstrate that transport intermediates containing ts-O45-G or endogenous PC I associate with different marker proteins *en route* to the Golgi complex. Altogether, our data provide strong evidence that trafficking of PC I and conventional secretory cargo between the ER and the Golgi complex differs at a molecular level.

Results

Controlled trafficking of endogenous PC I provides the basis for quantitative functional analysis

Being characterized by high expression levels of endogenous PC I, NIH 3T3 mouse fibroblasts provide a suitable environment to investigate the secretory pathway of this protein. In cells growing without ascorbate, essentially all PC I localizes to the ER as visualized by its colocalization to the ER-resident chaperone protein disulfide isomerase (PDI) (Figure 1A). After the addition of ascorbate (see *Materials and Methods*) and the subsequent stimulation of the folding reactions in the ER, PC I leaves the ER in a gradual manner and concentrates in the Golgi complex (Figure 1A). No significant loss of the total amount of the PC-I-specific fluorescence is occurring at this time (Figure 1B). Thereafter, the protein is sorted into post-Golgi carriers, which were defined as secretory vacuoles by electron microscopy studies (17,18), and it is secreted into the extra-cellular space. As a result of ascorbate treatment, PC-I-specific fluorescence is diminished from the cells; and the total time needed to secrete PC I completely is about 180 minutes (Figure 1B, black symbols). This is in good agreement to the secretion rates of PC I observed by electron microscopy in primary cells (17) and to the rates obtained by metabolic chase in cultured fibroblasts (19). Essentially, all PC I stay in the ER if no ascorbate is added (data not shown). Gradual disappearance of PC-I-specific fluorescence in the absence of ascorbate (Figure 1B, white symbols), most likely accounts for intracellular PC I degradation. Within a period of 180 minutes, this degradation reaches up to 30% of the total intracellular PC I, and is in good agreement with the data of biochemical chase experiments (20).

Upon entering the secretory pathway, PC I undergoes a secondary quality control with not properly folded molecules being degraded in the endosomal–lysosomal system (21). Distribution of the PC-I-specific post-Golgi carriers in relation to the markers of endosomes and lysosomes, namely transferrin receptor (TfR) (22) and lysosome-associated membrane protein 1 (LAMP1) (23), respectively, revealed little if any colocalization with PC I (Figure 1A). This indicates that the disappearance of PC-I-specific fluorescence in the presence of ascorbate largely occurs through secretion, and not by degradation.

Comparison PC I and ts-O45-G trafficking in mouse NIH 3T3 cells

The behaviour of PC I in NIH 3T3 cells was compared with that of ts-O45-G – a conventional marker widely used to investigate mechanisms of secretory membrane trafficking (24–26). Ts-O45-G is a temperature-sensitive variant of the vesicular stomatitis virus glycoprotein and has the feature of accumulating in the ER at 39.5°C, but moves to the plasma membrane (PM) at the permissive temperature of 32°C (27,28). Here, ts-O45-G was introduced into the cells by adenoviral infection, and its arrival to the PM was monitored by immunostaining using ts-O45-G-specific antibodies (see *Materials and Methods*). The maximum amount of ts-O45-G reached the PM in 60 minutes (Figure 1C) and decreased at later time-points possibly because of its internalisation and recycling (for review, see 29).

Next, the distribution of PC I and ts-O45-G-specific transport carriers in relation to several endogenous marker proteins was investigated. Taking into consideration, the differences in secretion rates (Figure 1B,C), colocalization experiments for each cargo were done separately. In addition, to follow comprehensively PC I and ts-O45-G trafficking between the ER and the Golgi complex, colocalization experiments were pursued within a time interval of 3–30 minutes after the shift to 32°C for ts-O45-G or the addition of ascorbate for PC I (Figure 2E,F). In agreement with earlier studies (14,30,31), the degree of colocalization of ts-O45-G and COPI changes as ts-O45-G progresses towards the Golgi complex, reaching a maximum of 60% after 15 minutes of ER release (Figure 2B,F). On the contrary, PC I-specific carriers showed less than 10% colocalization with COPI over the entire period of 30 minutes after the release of PC I from the ER (Figure 2A,E). Next, we performed colocalization experiments with the PC I-specific chaperone heat shock protein 47 (Hsp47) that is normally located in the ER and involved in the folding of PC I (32,33). The Hsp47 binds to and stabilizes the triple-helix of PC I (34), and extends its chaperone action by concomitant exit from the ER (33,35). Later, it dissociates from PC I either at intermediated compartment or at *cis* Golgi apparatus because of a change of lumenal pH and/or reduced concentration (33,36). As expected, PC I-specific structures largely colocalized to Hsp47 during the period of time needed to transport PC I from the ER to the Golgi complex (Figure 2C). The maximum of colocalization of 80% was determined at 7 minutes after ER release, and it was gradually decreased as PC I progressed towards to the Golgi complex (Figure 2E). Colocalization of Hsp47 and PC I occurred preferentially in structures at distance from the Golgi complex, with essentially no colocalizing of the two markers within the Golgi complex area (Figure 2C). On the contrary, no significant overlap was recorded between ts-O45-G and Hsp47 at any time-point tested (Figure 2D,F).

As both cargoes require different synchronisation procedures, we have tested the behaviour of each cargo in the reciprocal conditions. Neither rate of transport nor colocalization properties of ts-O45-G was affected by the addition of ascorbate (data not shown). On the contrary, by applying a 39.5/32°C temperature shift during the ER

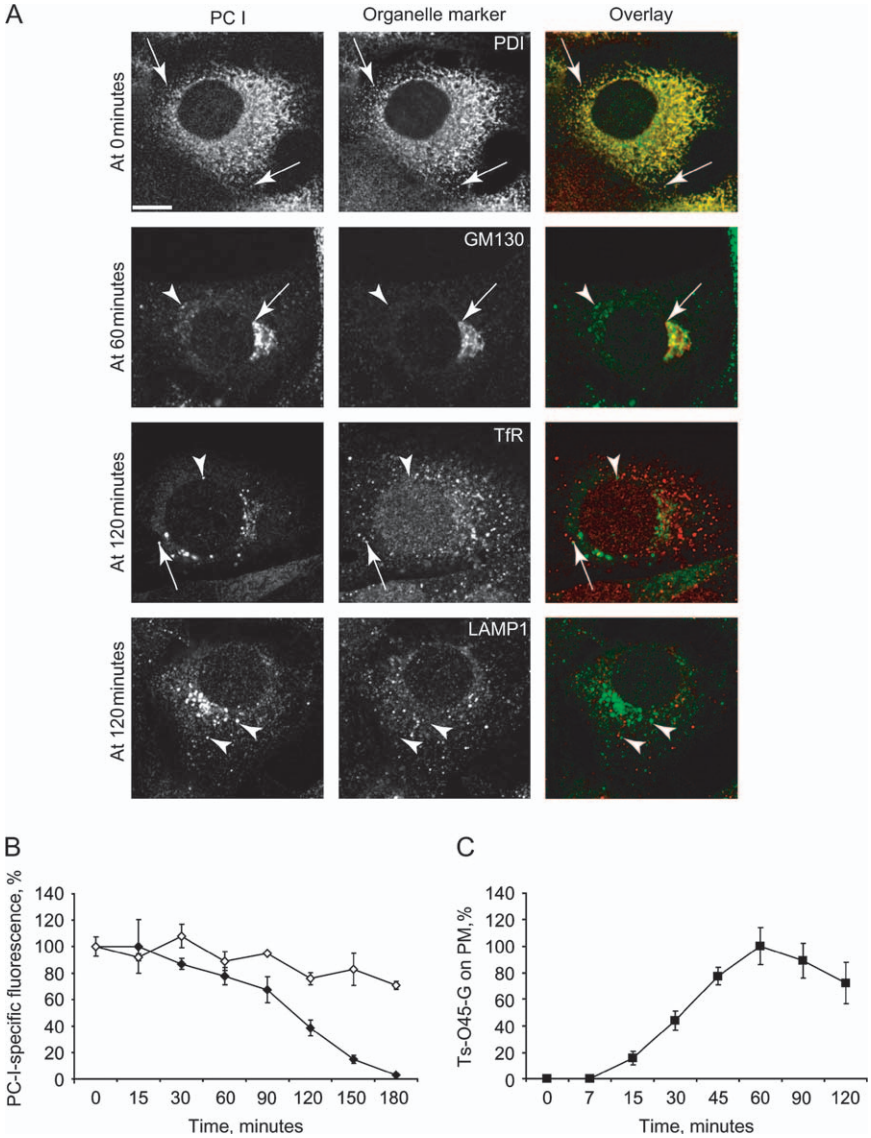

Figure 1: Secretion of PC I and ts-O45-G in NIH 3T3 cells. A) Trafficking of endogenous PC I after addition of ascorbate. Endogenous PC I is localized in the ER of non-treated cells as visualized by colocalization to ER-resident protein PDI. The addition of ascorbate induces folding and transport of PC I to the Golgi complex as visualized by colocalization to *cis* Golgi marker GM130. After passage through the Golgi complex, PC I is sorted into post-Golgi carriers and eventually secreted. No significant colocalization of PC I positive carriers to endosomes and lysosomes has been detected as visualized by colocalization to endosomal marker TfR and LAMP1, respectively. Arrows point to colocalizing structures, and arrowheads point to non-colocalizing structures. In overlay pictures, green colour represents PC I, red colour represents the respective organelle marker and yellow colour represents overlapping structures. Scale bar = 20 μm. B) PC I behaviour with and without the addition of ascorbate. The addition of ascorbate induces gradual secretion of PC I within the period of 120–180 minutes (black symbols). In cells non-treated with ascorbate, PC I is not folded, retained in ER (data not shown) and PC-I-specific fluorescence is gradually diminished possibly because of the intracellular degradation (white symbols). The *x*-axis represents time in minutes, *y*-axis represents intracellular amount of PC I as determined by immunostainings. PC-I-specific fluorescence is assigned as 100% in non-treated cells at time-point 0 minute. C) Rate of ts-O45-G trafficking. The *x*-axis represents time in minutes, *y*-axis represents amount of ts-O45-G, which reached PM as determined by immunostainings. Ts-O45-G-specific fluorescence is assigned as 100% when intensity of PM staining reached maximum (60 minutes). In both graphs (B and C) are shown mean values of 80–100 cells at each time-point, with bars indicating standard deviations.

exit of PC I severe inhibition of PC I secretion was obtained: about 60% of protein was still present in cells after 3 h of incubation and, largely, was still localized in the ER (data not shown). Probably, that indicates inhibition of the folding process in the ER, and corresponds well to the melting curves of PC I triple-helix, which denatures at the temperatures above 39°C and is not able to refold if temperatures are not below 25–30°C (37).

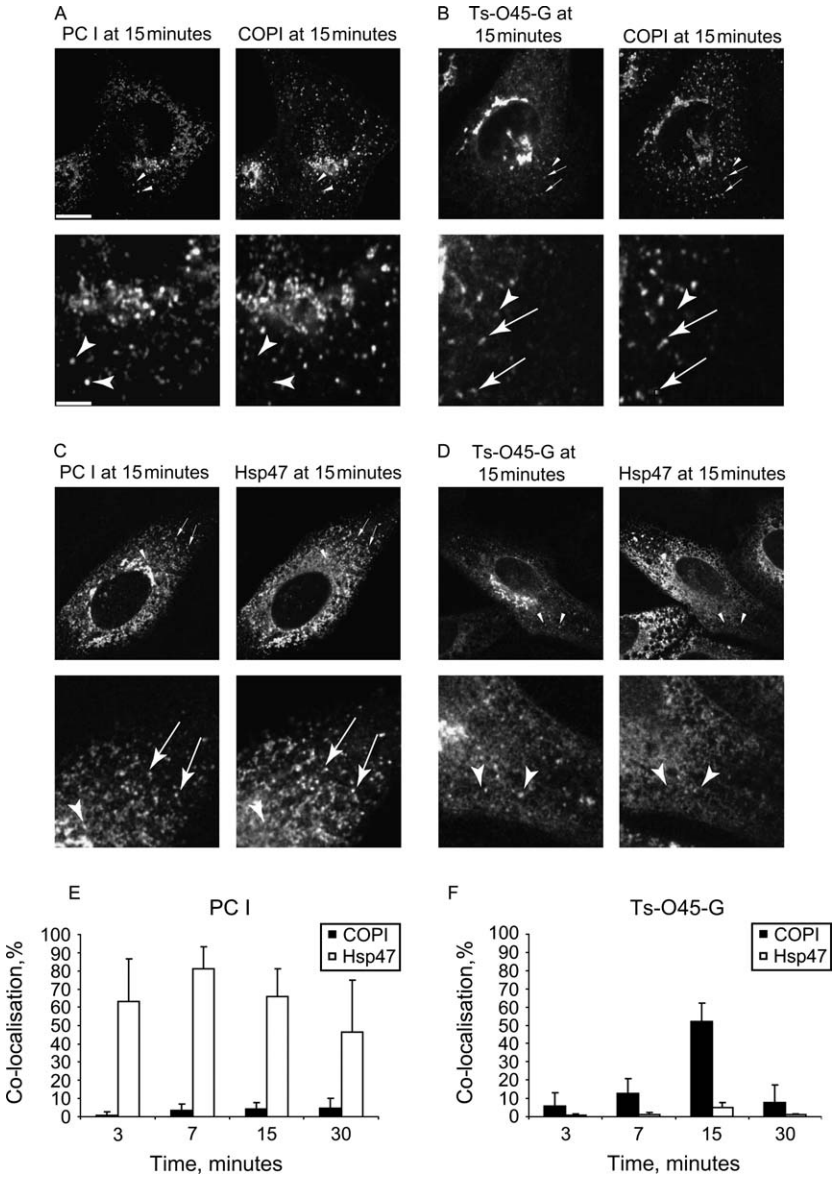

Figure 2: Colocalization of PC I and ts-O45-G-specific carriers with different markers. A) Colocalization of PC I and COPI, B) Colocalization of ts-O45-G and COPI, C) Colocalization of PC I and Hsp47 and D) Colocalization of ts-O45-G and Hsp47. Secretion of both cargoes was induced separately by the addition of ascorbate for PC I and by the temperature shift for ts-O45-G (see *Materials and Methods*). The images portray distribution of the cargo-specific structures and the respective markers 15 minutes after the ER exit. Images in the lower rows of A, B, C and D depict colocalizing and not colocalizing structures at a higher magnification. Arrows indicate colocalizing structures, and arrowheads indicate non-colocalizing structures. Scale bar = 20 μm in the upper images and 7 μm in the lower images. E) Quantitative colocalization of PC I with COPI and Hsp47. F) Quantitative colocalization ts-O45-G with COPI and Hsp47. Secretion of both cargoes was followed during first 3–30 minutes (*x*-axis) after the ER release. At each time-point, PC I-and ts-O45-G-positive structures were colocalized to endogenous COPI (black columns) and Hsp47 (white columns) (see *Materials and Methods*). Fraction of cargo-specific structures colocalizing to the particular marker was expressed as percents of colocalization (*y*-axis). At each time-point, mean values were calculated from 5 to 7 randomly chosen cells corresponding to 500–1000 structures; bars indicate standard deviations.

Functional PC I and ts-O45-G transport assays in NIH 3T3 cells

Recent work with ts-O45-G as a model cargo identified a number of GFP-tagged proteins that specifically interfere with its secretion when over-expressed (16). Here, we have developed a new quantitative assay to test how PC I secretion is affected when these GFP-tagged constructs are over-expressed.

For this, those GFP-tagged proteins, which inhibited ts-O45-G transport most strongly in the previous study, were chosen. As these 14 test molecules are human proteins, they were initially retested to influence ts-O45-G transport in NIH 3T3 cells (see *Materials and Methods*; Table 1). Both N- and C-terminal constructs of these molecules were assayed, when available. The test clones were over-expressed, incubated for 24 h and the arrival of ts-O45-G at the PM was measured 60 minutes after temperature shift to 32°C. Only when ts-O45-G trafficking was reduced by more than 20% in comparison with the non-transfected cells, the respective complementary DNA (cDNA)-GFP was classified as an effector (Table 1, bold numbers). All test constructs were confirmed to have an influence on ts-O45-G trafficking also in mouse 3T3 cells. Moreover, subcellular localization of cDNA-GFP clones in 3T3 cells was identical to those previously observed in HeLa and Vero cells (16; http://gfp-cdna.embl.de/). In addition, 12 clones have close homologs in mouse genome as could be determined by BLAST search, therefore possibly have analogous interaction partners and could be functionally incorporated into endogenous complexes. Two of the human proteins (AL136588 and CN155) have no identifiable

Table 1: Comparison of PC I and ts-O45-G transport assays in NIH 3T3 cells

Name and accession number	Function	Sub-cellular localization[a]		Ts-O45-G transport rate[b]		PC I retention[c]		Features
		N-terminal	C-terminal	N-terminal	C-terminal	N-terminal	C-terminal	
Soluble YFP		Cytoplasm–nucleus		0.99 ± 0.15[d]		0.83 ± 0.17		Soluble
Soluble CFP		Cytoplasm–nucleus		1.2 ± 0.25		0.91 ± 0.15		Soluble
Sar1-GTPase-YFP	Transport: regulation of ER exit (14)	ND	ER–Golgi apparatus	ND	**0.21 ± 0.03**	ND	**0.33 ± 0.22**	Soluble
Sar1-GTPase-CFP	Transport: regulation of ER exit (14)	ND	ER–Golgi apparatus	ND	**0.21 ± 0.21**	ND	**0.45 ± 0.22**	Soluble
USE1 AF220052	Transport: retrograde Golgi–ER transport(38)	ER–Golgi apparatus	ER–punct. str	**0.56 ± 0.07**	0.82 ± 0.16	0.89 ± 0.17	1.12 ± 0.07	One TM
SGTA AL050156	Unknown acts as a cochaperone (41)	Cytoplasm–nuclei		**0.68 ± 0.08**	1.22 ± 0.12	0.83 ± 0.2	0.84 ± 0.22	Soluble
PARM1 AL080121	Unknown	Golgi apparatus, PM, punct. str		**0.52 ± 0.18**	**0.44 ± 0.04**	**0.54 ± 0.27**	0.95 ± 0.28	Signal peptide, one TM
PAIRB AL080119	Unknown: binds to serpin messenger RNA (59)	Cytoplasm–Golgi apparatus		0.72 ± 0.19	**0.62 ± 0.18**	0.82 ± 0.18	0.86 ± 0.16	Soluble
AL136559	Unknown	Cytoplasm		0.85 ± 0.11	ND	0.86 ± 0.17	ND	Soluble
GOT1B AL136571	Transport homolog of Got1 family (44)	ER–Golgi apparatus		**0.71 ± 0.11**	**0.36 ± 0.15**	**0.58 ± 0.21**	0.89 ± 0.26	Four TMs
AL136588	Unknown	ER		**0.34 ± 0.14**	**0.26 ± 0.03**	1.05 ± 0.26	1.09 ± 0.17	Two TMs
SPAT7 AL136604	Unknown	MTs		**0.57 ± 0.16**	ND	**0.64 ± 0.19**	0.91 ± 0.09	Soluble
AL136618	Unknown	Cytoplasm		**0.67 ± 0.08**	ND	1.02 ± 0.18	ND	Soluble
gamma-BAR AL136628	Transport: AP-1 regulation at TGN (40)	Cytoplasm–nuclei	Golgi apparatus–PM–punct. str	ND	**0.63 ± 0.13**	ND	**0.55 ± 0.31**	Soluble
p34 AL136715	Transport: interaction with AP-1 and AP-2 (46)	Cytoplasm		0.86 ± 0.31	ND	**2.2 ± 0.33**	ND	Soluble
ALG9 AL136927	Protein modification: mannosyl-transferase (60)	ER		0.91 ± 0.14	ND	0.92 ± 0.1	ND	Eight TMs
VMP1 AL136711	Apoptosis: inducers vacuole formation (61)	ER–Golgi apparatus	ND	ND	ND	**0.42 ± 0.35**	ND	Six to seven TMs
CN155 AL136775	Unknown	Cytoplasm		**0.48 ± 0.15**	0.81 ± 0.09	0.91 ± 0.23	0.88 ± 0.22	Soluble
AL136916	Unknown	Golgi apparatus–punct. struc		**0.54 ± 0.29**	**0.41 ± 0.04**	**0.47 ± 0.33**	0.88 ± 0.14	Four TMs
YIPF1 AL713668	Transport: homolog of Yip1 family (62)	ER–Golgi apparatus, punct. struc		**0.57 ± 0.06**	**0.44 ± 0.07**	**0.24 ± 0.16**	1.14 ± 0.22	Five TMs
PACN1 AL834211	Transport: regulates endocytosis (63)	Cytoplasm		1 ± 0.13	ND	0.88 ± 0.19	ND	Soluble
CD016 BC009485	Transport: isoform of gamma-BAR (40)	Cytoplasm–nuclei	Golgi apparatus–PM–punct. struc	ND	ND	**0.51 ± 0.21**	**0.4 ± 0.13**	Soluble

ND, not determined; punct. str, punctuate structures; MTs, microtubule network.
[a]All clones exist in two variants: CFP fused to the N-terminus and YFP fused to the C-terminus.
[b]Ts-O45-G transport rate is expressed as a normalized transport ratio of transfected to non-transfected cells (for more details, see *Methods*).
[c]The PC I retention is expressed as a normalized retention of transfected to non-transfected cells and inverted (for more details, see *Methods*).
[d]Normalized average value and propagating error of ratio derived from individual experiments.

homologs in the mouse genome so far, although they interfere with the transport of ts-O45-G. Presumably, their mouse counterparts preserve similar structure and, consequently, function, but diverge on a level of amino acid sequence.

Next, the cDNA-GFPs were further exploited to quantitatively determine their influence on the secretion of PC I. For this, PC I secretion was synchronized by the addition of ascorbate, and remaining PC I-specific fluorescence was imaged after 120 minutes and compared between transfected and non-transfected cells (see *Materials and Methods*). As negative and positive controls soluble cyan fluorescent protein (CFP)/yellow fluorescent protein (YFP) and CFP/YFP-tagged dominant-negative Sar1p [SAR1p$^{[H79G]}$; (14)] were used. In cells expressing soluble CFP, transport of PC I occurred with an efficiency similar to that observed in neighbouring non-transfected cells (Table 1; see *Materials and Methods*). In contrast, when SAR1p$^{[H79G]}$ was over-expressed, the amount of PC I transported was decreased fivefold. Comparable effects were also obtained for ts-O45-G, thus indicating the functionality of the PC I transport assay.

Assessment of PC I secretion rates in the conditions of over-expression of the 14 test cDNA-GFPs identified six proteins that had no influence on PC I secretion (USEI, SGTA, PAIRB, AL136588, AL136618 and CN155) (Table 1 and Figure 3A). These results were obtained by measuring PC I secretion at 120 minutes after addition of ascorbate. In order to characterize the influence of these molecules on PC I secretion more accurately, they were tested over the broader time scale of 90–180 minutes. No interference of the over-expression of these cDNA-GFPs with PC I secretion was observed at any time-point tested (Figure 3 B). Eight cDNA-GFPs (PARM1I, GOT1B, SPAT7, gamma-BAR, VMP1, AL136916, YIPF1 and CD016) were assigned to inhibit the secretion of PC I when over-expressed (Table 1). Over-expression of these cDNAs reduced the secretion of PC I, which could be detected as the remaining PC I-specific fluorescence at the Golgi complex or post-Golgi structures at time-points of 120–150 minutes (Figure 3A). At the later stages of PC I progression (180 minutes), essentially all transfected cells no longer contained PC I-specific fluorescence. Over-expression of two cDNA-GFPs, namely YIPF1 and VMP1, induced a persistent block of PC I secretion (Figure 3A). This was characterized by an accumulation of PC I-specific fluorescence in the Golgi complex region in the transfected cells, which did not disappear at later time-points.

In addition to the inhibiting molecules, four cDNA-GFPs (ALG9, AL136559, P34 and PACN1) without effect on the transport rate of ts-O45-G (16) were tested in the PC I secretion assay. Three of those molecules had no effect (ALG9, AL136559 and PACN1), but one clone, namely P34, increased the secretion of PC I by more than 50% (Table 1). Additional tests were done to assay whether over-expression of P34 influences the intracellular amounts of PC I, and whether the chase of cells without the addition of ascorbate leads to the significant decrease of PC I. Both tests were negative (data not shown), leading to the conclusion that over-expression of P34 indeed facilitates the secretion of PC I, without influencing the degradation or synthesis rates.

To check whether different trafficking requirements for ts-O45-G and PC I do not account for differences in their intracellular amounts, and, thus, different requirements for some components and not the others, we have compared how transport efficiency of ts-O45-G depends on its expression levels. As shown in the Figure 4, both in non-transfected and in transfected cells, there is a reverse correlation between the transport rate and the expression levels of ts-O45-G. Despite that, in case of ts-O45-G being inhibited or not, this is reflected at any expression level of this cargo. For instance, ts-O45-G trafficking is inhibited by the over-expression of USEI and YIPF1 even when amount of ts-O45-G is low (constitutes not more than 30% of the relative ts-O45-G expression level) (Figure 4). Taken into consideration that PC I is a highly abundant and evenly expressed protein in mouse fibroblasts, non-interference with its secretion under conditions of over-expression of some cDNA-GFPs rather account for different molecular requirements than differences in the intracellular amounts of PC I.

In order to test whether the differential effects of over-expressed cDNAs on ts-O45-G and PC I trafficking are not because of the different experimental conditions (temperature), we repeated the ts-O45-G transport assay at 37°C. At 37°C, ts-O45-G transport (see *Materials and Methods*, for details) was less efficient as expected (data not shown). Nevertheless, over-expression of cDNAs also inhibited its transport, although slightly less efficient as in experiments performed at 32°C. Expression of SAR1p$^{[H79G]}$ resulted in a normalized ts-O45-G transport of 0.58 ± 0.13 at 37°C compared with 0.21 ± 0.21 at 32°C; expression of CFP resulted in a normalized transport of 0.9 ± 0.08 at 37°C compared with 1.2 ± 0.25 at 32°C; expression of USEI resulted in a normalized transport of 0.77 ± 0.11 at 37°C compared with 0.56 ± 0.07 at 32°C and expression of AL136588 resulted in a normalized transport of 0.58 ± 0.04 at 37°C compared with 0.34 ± 0.14 at 32°C.

The majority of proteins without the effect on PC I secretion – four of six – are soluble and localize to cytoplasm (SGTA, PAIRB, AL136618 and CN155); remaining two proteins bear one to two TM domains (USE1 and AL136588). On contrary, six of eight proteins, which retarded PC I secretion contain various numbers of TM domains and localize to ER, Golgi complex and punctate structures (Table 1). Among the hits specific for both cargoes or only for ts-O45-G, various characterized or putative members of the transport machinery are found.

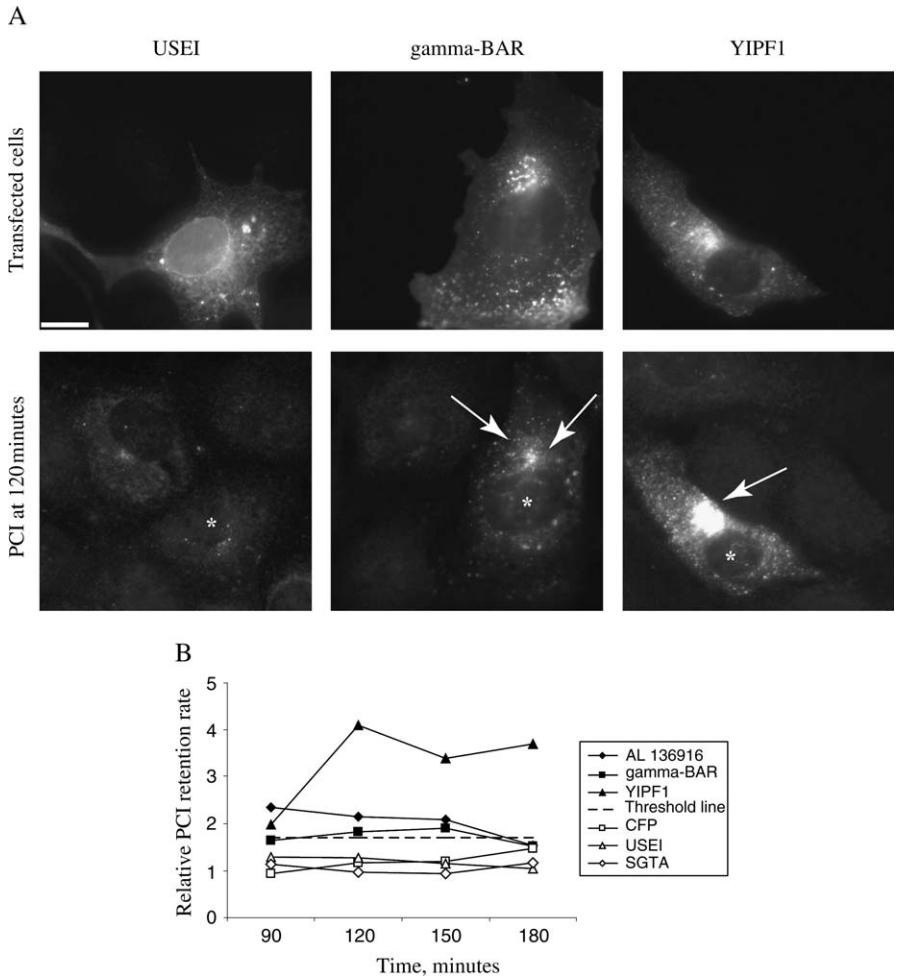

Figure 3: PC I tranport assay in NIH 3T3 cells. A) Examples of intracellular PC I retention caused by the over-expression of cDNA-GFP. Cells were transfected with the cDNA-GFP constructs, incubated for 24 h, and secretion of PC I was induced by the addition of ascorbate. Over-expression of a putative Golgi complex-ER SNARE USEI has no effect on PC I secretion (left column). The PC I progression through Golgi complex and/or sorting into post-Golgi carriers is slowed down by over-expression of gamma-BAR (middle column). Over-expression of a putative Rab effector YIPF1 blocks PC I secretion in the Golgi complex (right column). Asterisks indicate transfected cells, and arrows point to PC I retarded in sub-cellular structures of the secretory pathway. Scale bar = 10 μm. B) Effect of cDNA-GFP over-expression on PC I secretion as a function of time. Here, residual amounts of PC I were visualized at different time-points after the addition of ascorbate (*x*-axis). Amounts of PC-I-specific fluorescence in transfected cells were compared with that in non-transfected cells at each time-point separately, expressed as a normalized ratio of PC I retention rate (*y*-axis) (for details, see *Materials and Methods*). Lines with the black symbols indicate cDNA-GFPs, which retarded PC I secretion when over-expressed; lines with the white symbols indicate cDNA-GFPs, which caused no effect on PC I secretion. The threshold separating normal and affected PC I secretion is indicated as a dashed line and was determined as described in *Materials and Methods*.

For example, among proteins without the effect on PC I secretion is USEI – a putative orthologue of the yeast retrograde ER–Golgi SNARE (38); or SGTA – a molecular chaperone involved in the folding and/or secretion of various proteins (39).

Assignment of intracellular site of action of cDNA-GFPs

In order to find more commonalities between the molecules with and without an effect on PC I secretion, we next designed experiments to characterize where these molecules act in the secretory pathway when over-expressed. For this, the fraction of ts-O45-G associated with the Golgi complex at different time-points after the shift to 32°C was measured. The overall effect was expressed as a difference between the mean values of non-transfected and transfected cells. The difference was only considered to be significant when the pooled standard error of the difference was greater than 2 (Figure 5A,B; see *Materials and Methods*). The results of these experiments are summarized in Figure 5 and Table 2.

Six cDNAs had an effect on ts-O45-G transport starting at the 5–10 minutes after the ER exit (Figure 5A). For two

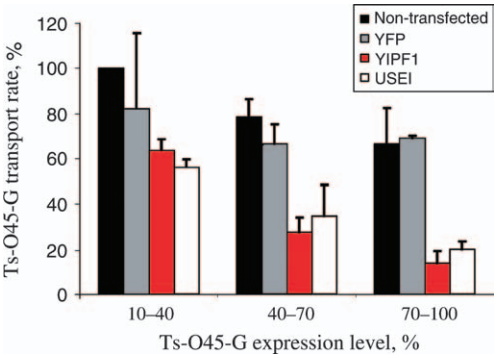

Figure 4: Correlation between ts-O45-G transport rate and expression level. The data of the ts-O45-G secretion assay under conditions of cDNA-GFPs over-expression were used to correlate cargo transport rate to its expression level. Transport rate of ts-O45-G in non-transfected cells (black), transfected with CFP (grey), transfected with of a putative Rab effector YIPF1 (red) and transfected with a putative ER SNARE USEI (white) are represented in *y*-axis. Transport rate in the transfected cells was normalized to the transport rate in non-transfected cells for each experiment. Intracellular amounts of relatively expressed ts-O45-G are represented in *x*-axis. Accordingly, three groups of cells are separated, namely with low ts-O45-G expression level (10–40%), with middle ts-O45-G expression level (40–70%) and with high ts-O45-G expression level (70–100%). Over-expression of the inhibiting molecules, such as YIPF1 and USEI, exerts their action on the secretion rate of ts-O45-G already at the low levels of cargo protein. For each experiment, mean values of ts-O45-G secretion rate were calculated from about 100 cells; bars indicate standard deviations.

cDNA-GFPs, namely GOT1B and YIPF1, the determined site of the action correlates well with the sub-cellular localization (ER, Golgi complex) and predicted functional roles in the early events of the membrane trafficking. The other three cDNAs are essentially uncharacterized proteins localized to the ER (AL136588) and cytoplasm (AL136618 and PAIRB) (Table 2). Two proteins (PARM1I and AL136916) appear to act later (20–30 minutes after the ER exit), and potentially could indicate their function within the Golgi complex. Both of them are novel proteins with TM regions and localize to the Golgi complex and punctate structures. Finally, three cDNA-GFPs interfered with the late steps of ts-O45-G secretion (30–60 minutes after the ER exit) (gamma-BAR, SGTA and CN155) (Table 2 and Figure 5B,D). Similar to GOT1B and YIPF1, gamma-BAR serves as a positive control of the method, being localized to the structures of the late secretory pathway and acting on the carriers formation at the *trans*-Golgi network (TGN) (40). The SGTA could also potentially be involved in the trafficking events between the Golgi complex and the PM by being involved in the formation of the clathrin-coated carriers (41).

These data suggest that the cDNA-GFPs, which affect ts-O45-G transport when over-expressed act on various different steps of the secretory pathway. The molecules without any effect on PC I secretion are players in the early (5–10 minutes) (PAIRB, AL136588 and AL136618) or late (60 minutes) (SGTA and CN155) trafficking events (Figure 5 and Table 2). This in turn supports the idea of the presence of differential cargo-sorting mechanisms not only at the TGN but also at the pre-Golgi level.

To obtain independent evidence for the site of action of the cDNA-GFPs, we next investigated which structures/markers of the secretory pathway were affected when these clones were over-expressed (Figure 6). Consistent with the functional data described above, cDNA-GFPs that inhibited ts-O45-G trafficking at the late and middle time-points induced changes in the distribution of endosomal or TGN markers, but not those markers highlighting the early secretory pathway (e.g., AL136916 in Table 3). On the contrary, cDNA-GFPs that inhibited the progression of ts-O45-G at early time-points induced the redistribution of early markers such as ERGIC53, COPI and COPII (e.g., GOT1B, YIPF1 in Table 3).

Differential transport of PC I and ts-O45-G under conditions of downregulation of components of the early secretory pathway

In order to further investigate possibly different requirements for PC I and ts-O45-G secretion during ER to Golgi trafficking, we followed transport of these cargoes under the conditions of downregulation by RNAi of well-characterized proteins acting in the early secretory pathway.

At first, we have optimized experimental conditions by measuring depletion rates of Hsp47 and COPI under various time periods of incubation (12, 24, 48 and 72 h) with the respective small interfering RNAs (siRNAs). For each protein, two siRNAs were used. The efficiency of the downregulation effect was quantitatively assessed by immunostainings of individual cells and in cell lysates by Western blots (Figure 7B,C,D,E). Intracellular amounts of COPI were reduced by downregulating one of its constituents, namely β-COP. The amounts of β-COP-specific immunostaining correlated well with the incubation time of the respective RNAis to downregulate β-COPI, being in the range of 70% after 12 h of incubation, 50–60% after 24 h and 30–10% after 48 and 72 h in comparison to the non-treated cells (Figure 7C). However, conditions when β-COP was downregulated efficiently (e.g., more than 24 h of incubation) induced profound alterations in the morphology of the structures decorated by this molecule. Essentially, the same was obtained by downregulating β′-COP (data not shown). For the efficient downregulation of Hsp47 (up to 50–90%), 48 h of incubation with the respective siRNAs was also necessary (Figure 7B,D). In contrast to the experiments with COPI downregulated, reduction of intracellular Hsp47 caused no apparent morphological changes of the early secretory pathway. Next, we performed quantitative PC I and ts-O45-G secretion assays under the conditions of downregulation by siRNAs

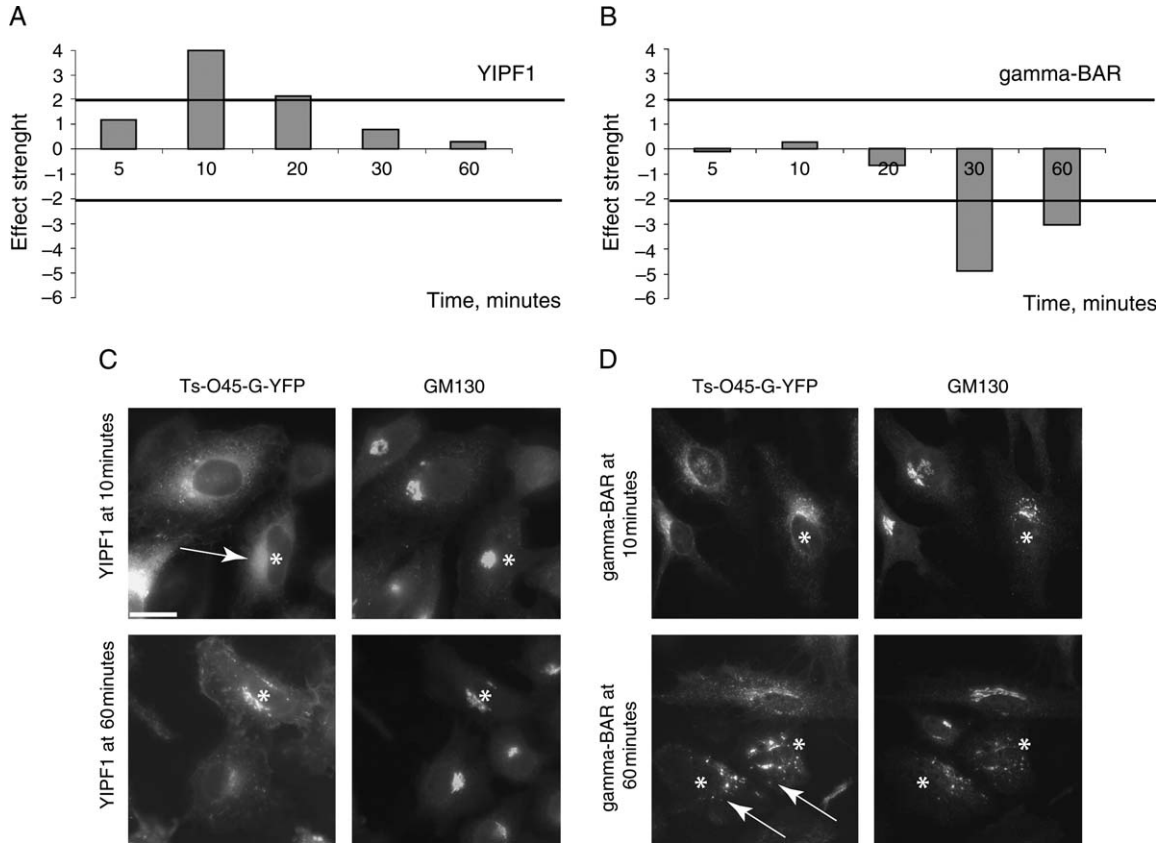

Figure 5: Intracellular site of action of cDNA-GFPs. A and B) Strategy to assign inhibition of ts-O45-G trafficking to specific intracellular sites. HeLa cells were transfected with cDNA-GFP constructs and incubated for 24 h. Ts-O45-G was accumulated in the ER, released by the temperature shift, and its trafficking to the PM was imaged at the different time-points, depicted on *x*-axis in every graph. The total amount of ts-O45-G produced in cells was compared with that passing the area of the Golgi complex at every time-point. The fraction of ts-O45-G residing in the Golgi complex was compared between non-transfected and transfected cells. The resulting difference was named 'effect strength', depicted on the *y*-axis and was considered to be significant only when a pooled standard error of the difference was bigger than 2 (straight lines in each graph). Positive values on the *y*-axis indicate that fraction of ts-O45-G at the Golgi complex is higher in non-transfected cells, and the negative values indicate the opposite. C) The example of ts-O45-G transport retardation during the early trafficking events. Over-expression of a putative Rab effector YIPF1 apparently affects early steps in ts-O45-G trafficking (10–20 minutes after the ER exit). D) The example of ts-O45-G transport retardation during the late trafficking events. Over-expression of gamma-BAR has no effect on the early steps of ts-O45-G secretion, but traps ts-O45-G in the Golgi complex at 30–60 minutes after the ER exit. Asterisks indicate transfected cells, and arrows indicate transfected cells with the impaired progression of ts-O45-G-YFP. Scale bar = 20 μm.

of several other components of the early secretory pathway and other constituents of COPI coat (Figure 7A). In order to compromise between the conditions of sufficient protein depletion and the intact morphology of the early secretory pathway, all experiments were done after incubation with siRNAs at two time-points, namely for 24 and 48 h.

The essential role of COPI in ts-O45-G transport was confirmed by a considerable inhibition of ts-O45-G transport rate when β-COP and ARF1 were downregulated. Ts-O45-G passage through the secretory pathway was inhibited when the morphology of the secretory pathway was still intact, and the downregulation of intracellular amount of COPI were little (e.g., 24 h of incubation with siRNAs against β-COP). On contrary, no inhibition of PC I secretion could be observed under these conditions (Figure 7A). In addition, differential effects on PC I and ts-O45-G were obtained in the experiments when KDEL receptor (KDEL-R) and a putative fusion factor to the Golgi complex GOT1B were downregulated. As a primary effect, Hsp47 downregulation by both siRNAs used induced a corresponding reduction of PC I expression level (data not shown). This is in an agreement with the numerous observations that Hsp47 and PC I intracellular amounts are regulated on levels of transcription and translation in the normal and pathological conditions (for review, see 36). No significant changes in trafficking of PC I was observed under these conditions when the normalized values were compared with those of untreated cells (Figure 7A). In good agreement with the colocalization data (Figure 2B,F), no changes in the expression levels and transport rates of

Table 2: Classification of cDNA-GFPs according to where they inhibit the transport of ts-O45-G

Name and accession number	Time-points at which ts-O45-G passage through the Golgi complex was disturbed (minutes)	Localization
Early and middle		
AL136618	5	Cytoplasm
AL136588	5–30	ER
VMP1 AL136711	5–60	ER, Golgi apparatus
PAIRB AL080119	10	Cytoplasm
YIPF1 AL713668	10–20	ER, Golgi apparatus, punct. str
GOT1B AL136571	10–30	ER, Golgi apparatus
Middle		
PARM1 AL080121	20	Golgi apparatus, PM, punct. str
AL136916	20	Golgi apparatus, punct. str
Middle and late		
gamma-BAR AL136628	30–60	Golgi apparatus, PM, punct. str
SGTA AL050156	60	Cytoplasm
CN155 AL136775	60	Cytoplasm
Early and late		
SPAT7 AL136604	5 and 60	MTs
Non-identified		
USE1 AF220052	None	ER, Golgi apparatus, punct. str

punct. str, punctate structures; MT, microtubule network.

ts-O45-G were observed when Hsp47 was downregulated. Finally, the essential role of COPII complex was demonstrated by downregulation of one of the component of COPII coat, namely Sar1a GTPase. This induced inhibition of both cargoes (Figure 7A).

Discussion

The membrane glycoprotein of vesicular stomatitis virus [ts-O45-G; (28)] has been extensively used in the past as a model membrane protein to study molecular aspects of the early and late secretory pathway (25,27,30,42). The transport features of this marker were thus used to conceptualize the secretory trafficking pathway in mammalian cells, particularly during the early secretory events. For instance, ts-O45-G exits the ER at COPII-coated ER exit sites (14), and progresses to the Golgi complex in carriers decorated by the COPI complex (30,43). Recent studies with PC I as an example of large cargo provided good evidence for alternative transport pathways between the ER and the Golgi complex. The GFP-tagged PC I is transported to the Golgi complex in carriers, which are not COPI coated (12). It has been proposed that it exits the ER at sites devoid of COPII (13), although the function of COPII appears to be required for ER exit (15). In contrast to the work by (12,13) suggested that ts-O45-G and PC I move together from the ER to the Golgi apparatus on the same complex carriers. In this study here, we performed experiments addressing these seemingly contradicting data and provide strong evidence that PC I and ts-O45-G have common but also different molecular requirements during pre- and post-Golgi trafficking events.

Recently, we identified novel human proteins that interfere with transport of ts-O45-G to the PM when over-expressed in intact cells (16). In order to compare the effect of these molecules on the trafficking of both cargoes, ts-O45-G and PC I, we have developed a quantitative assay to examine the secretion of PC I in mouse fibroblasts. From 25 ts-O45-G transport effectors identified earlier, we have chosen 14, which inhibited ts-O45-G secretion more than 50%. Quantitative analyses of PC I transport revealed that only 6 of these 14 proteins had an inhibitory effect on PC I and ts-O45-G transport. For instance, secretion of both cargoes was affected by the over-expression of GOT1B – a human orthologue of the yeast GOT1P protein, which has been described as being involved in the fusion of anterograde carriers to the *cis* Golgi network (44). Among the proteins that inhibited ts-O45-G transport but had no effect on PC I secretion are the putative Golgi to ER retrograde SNARE USE1 (38) and the molecular chaperone SGTA (39). These data clearly indicate that the trafficking routes of ts-O45-G and PC I have common but also different molecular requirements; and additional tests revealed that observed differences do not account for the different expression level of ts-O45-G and PC I. A putative influence of the different synchronisation protocols could also be largely excluded (see *Results*).

In order to characterize the test clones further, we have grouped them according to their intracellular sites of action. For this, we developed a quantitative approach to measure the rate with which ts-O45-G reaches and passes the Golgi complex. These measurements corresponded well with the predicted function of the proteins when available, their sub-cellular localization, and the alteration of well-characterized endogenous markers when the test proteins were over-expressed. In the case of the proteins localizing to the cytoplasm (4) or cytoskeleton (1), the assigned site of action serves as a primary spatial information for their intracellular function. For example, cytoplasmically localized SGTA protein inhibited ts-O45-G secretion at the late time-points, and this corresponds well to its proposed function of being involved into the formation of clathrin-coated carriers (41).

Interestingly, our experiments revealed that those proteins affecting ts-O45-G trafficking between 20 and 30 min after ER exit of the marker inhibited also PC I secretion. This

correlates nicely with the data suggesting that PC I and ts-O45-G are transported through the Golgi complex together (45). Differences between ts-O45-G and PC I secretion occurring during the late trafficking events could be exemplified by the behaviour of the P34 molecule. This cDNA encodes the p34 protein, which was shown by yeast two-hybrid analyses to bind adaptor protein 1 (AP-1) and AP-2 vesicular complexes (46). The p34 did not influence ts-O45-G arrival at the PM, but significantly facilitated PC I secretion (Table 1). These data most likely exclude the possibility that the observed differences between ts-O45-G and PC I trafficking in our functional assays result from an unspecific route taken by ts-O45-G, which could possibly occur because of high levels of ts-O45-G passing the secretory pathway in a synchronized manner. As a result, a specific pathway could be over-saturated and ts-O45-G missorted. On the contrary, with PC I being a natural cargo, cells would be well adapted to the high amounts of this molecule passing the secretory pathway. In the light of these type of events, the observation that PC I and ts-O45-G are transported in the same type of carriers (47) could possibly reflect aberrant ts-O45-G sorting. This would explain the data that these carriers are not coated with adaptor complexes despite the presence of basolateral cargo ts-O45-G (47); or that TGN exit of ts-O45-G in fibroblasts requires dynamin, despite that this protein regulates the apical transport route otherwise (48). It is important to note that our assays were done with only little to moderate amounts of ts-O45-G in cells, therefore our data possibly reflect most likely a differential behaviour of various cargoes in the conditions close to physiological ones.

Of the proteins acting on the early trafficking events, three (GOT1B, VMP1 and YIPF1) interfered with the secretion of both cargoes, another three (PAIRB, AL136588 and AL136618) affected ts-O45-G, but not the secretion of PC I. To complement our functional studies, suggesting that ts-O45-G and PC I exploit a differential molecular machinery for the early transport steps, we performed a number of colocalization experiments with endogenous markers. In agreement to previous data (12), little if any colocalization between carriers containing PC I and COPI was detected, whereas those carrying ts-O45-G showed more than 60% of colocalization with COPI. Experiments done under identical conditions with the recycling collagen-specific chaperone Hsp47 demonstrated a very high degree of colocalization of PC I and Hsp47 *en route* to the Golgi complex. On the contrary, ts-O45-G showed no colocalization with Hsp47 at any time-point after ER exit. Differential localization data of two markers over the entire period of time needed to transport them from the ER and Golgi complex (3–30 minutes) points out that segregation of these two markers occurs not only during ER exit but is also maintained during the following trafficking.

A very strong support for differential trafficking routes of ts-O45-G and PC I was obtained by the measurements of secretion rates of both cargoes, under conditions of down-regulation by RNAi of well-characterized proteins of the early secretory pathway. An intimate functional relation between PC I and Hsp47 was demonstrated by an altered expression level of PC I when Hsp47 was diminished. Reduction of Hsp47 resulted in simultaneous downregulation of PC I. This results confirms previous observations that Hsp47 and PC I intracellular amounts are transcriptionally and translationally coregulated (for review, see 36). Therefore, it appears that the necessity of Hsp47 in the biogenesis of PC I is on the level of events upstream membrane trafficking (transcription and translation). The proper adjustment of Hsp47 and PC I intracellular amounts might be crucial to ensure secretion of functional properly folded PC I. In contrast, production and secretion of not well folded PC I might occur under conditions of Hsp47 downregulation. Along these lines, it was recently reported (49) that PC I is produced and secreted in *Hsp47−/−* cells, but fail to undergo normal processing and fibrillogenesis. Functional irrelevance between Hsp47 and ts-O45-G was confirmed by the fact that the rate of ts-O45-G secretion and expression levels remained unchanged under the conditions of Hsp47 downregulation.

Further, ts-O45-G transport was clearly inhibited under the conditions of partial COPI downregulation, when no crucial changes of the early secretory pathway had occurred yet. Interestingly, secretion of PC I remained unaffected under these conditions, what clearly suggests that PC I secretion does not require COPI function or requires in a different way as described for ts-O45-G and is in good agreement with previous localization data (12) and those presented here. Additional confirmation of differential molecular requirements of both cargoes was obtained by down-regulating KDEL-R; Golgi complex to ER recycling of this protein was closely attributed to the functionality of COPI (50). Similar to experiments with COPI, no interference with the secretion of PC I was observed when KDEL-R was downregulated. However, a complete abrogation of the PC I secretion was observed at later stages of β-COP downregulation, which could rather be attributed to a general perturbation of the early secretory pathway, than direct functional relevance. Even under these conditions, ts-O45-G and PC I behaved differently, namely PC I remained localized in the ER, while ts-O45-G translocated into punctate post-ER structures or Golgi complex (data not shown). This is in a good agreement with earlier observations when COPI function was compromised by over-expressing ARF1 GTP mutant or by injecting specific antibodies inhibiting COPI function (15). The differential requirement for PC I and ts-O45-G ER to Golgi trafficking was also shown by assaying effects caused by down-regulation of a putative fusion factor to the *cis* Golgi complex GOT1B (44). As GOT1B and KDEL-R are both TM protein, these results suggest a possibility that not only regulatory but also mechanistic aspects of trafficking of ts-O45-G and PC I might be different. Finally, inhibition of ts-O45-G and PC I trafficking when Sar1a GTPase was downregulated indicates the necessity of COPII complex.

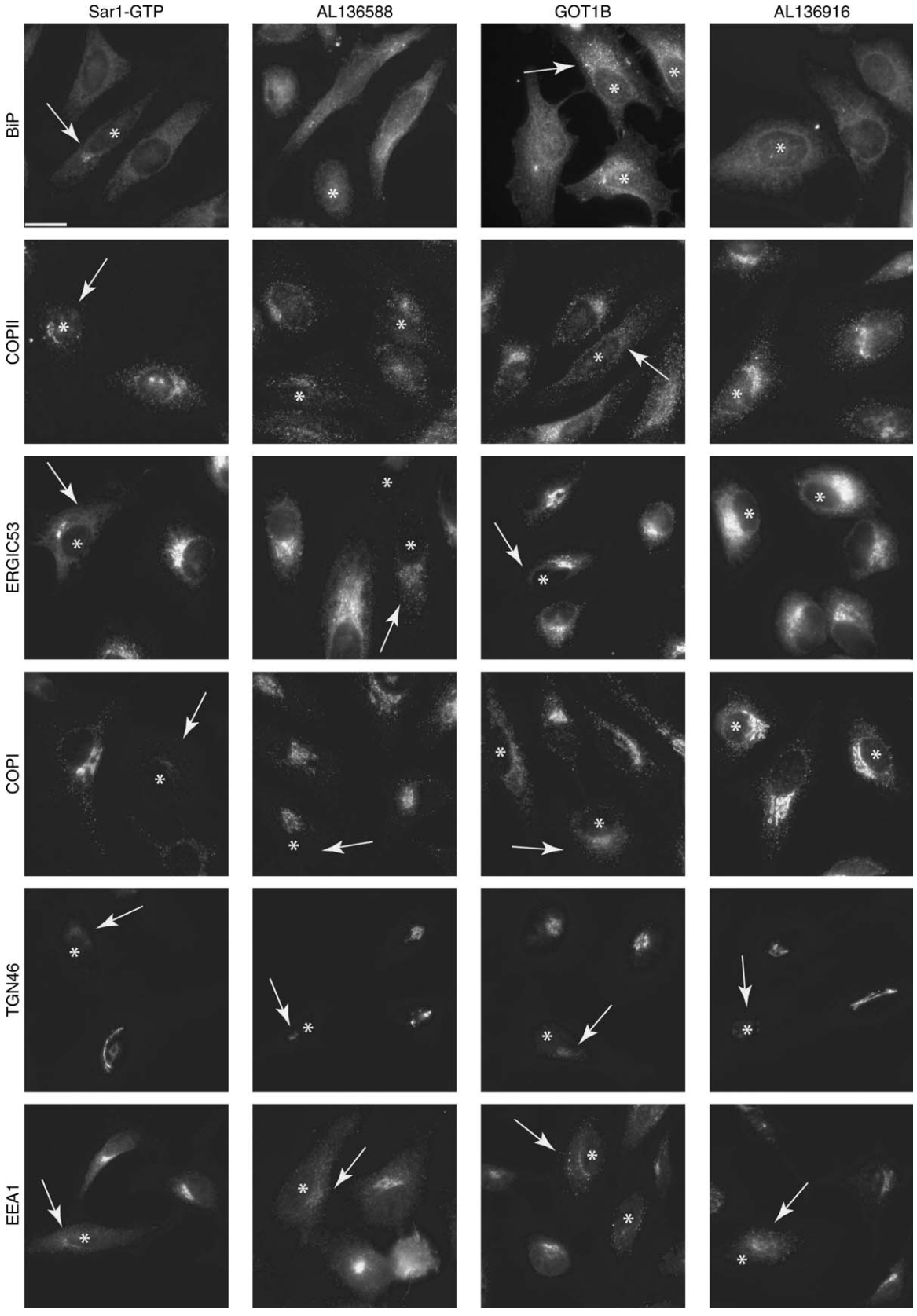

Figure 6: Legend on next page.

Table 3: Changes of the secretory pathway under the conditions of over-expression of cDNA-GFPs

Name and accession number[a]	BiP	COPII	ERGIC53	COPI	GM130[b]	TGN46	EEA1
Positive control							
Sar-GTP	++	++	++	++	+	++	+
Inhibits only ts-O45-G trafficking							
AL136588	−	−	+	+	++	++	+
USEI	−	−	−	−	+	+	−
AL136618	−	−	−	−	−	−	−
PAIRB	−	−	−	−	++	−	−
Inhibits ts-O45-G and PC I trafficking							
GOT1B	+	+	+	+	+	+	+
YIFP1	−	−	+	+	++	−	−
AL136916	−	−	−	−	−	++	+
Negative control							
CFP	−	−	−	−	−	−	−

++, over-expression of these clones induces disappearance of the respective markers from their normal sub-cellular localizations; +, over-expression of these clones induces redistribution of the respective markers.
[a]The cDNA-GFPs with the effect on the early steps of the ts-O45-G transport were taken for the analysis.
[b]Data taken from (16).

Our results are in a good agreement with recent observations that mutations in other COPII subunits, namely, Sec23a – the protein activating GTPase activity of Sar1a, cause an abnormal secretion of collagens (51,52), and that Sar1a-GDP or Sar1a-GTP mutants inhibit secretion of both cargoes (13,15). In contrast, functional performance of COPII complex might be different in respect to various cargoes. How these data correlate with the observation that ts-O45-G and PC I exit ER at the adjacent sites (13) remains to be investigated.

Taken together, our data show that ts-O45-G and PC I trafficking routes between the ER and the Golgi complex share some common features, but also differ considerably. It is likely that the differential entry into the secretory pathway originates already during the folding reactions because of the different kinetics or different chaperones involved. Further on, the segregation of cargo upon ER exit could rely on the presence of exit signals (e.g., C-terminal di-acidic stretch in the case of ts-O45-G) and a following active concentration of cargo. Meanwhile, the remaining signal-free proteins (PC I in this case) could use rather passive mechanisms like *en block* protrusion (13) to exit the ER. In addition, the composition, size and abundance of cargo proteins could also be deciding factors for the differential behaviour. Our data favour the idea that further segregation is secured by the formation and progression of different types of carriers. Presumably, the ones containing actively packed cargo such as ts-O45-G also contain a lot of components of the trafficking machinery, which is returned back in a COPI-dependent fashion. On the contrary, when specialized and abundant cargo, such as PC I, exits the ER and enters the secretory pathway passively such cargo might be the essential constituent of transport carriers. Consequently, the absence of the extensive retrograde flow from these carriers would explain non-colocalization to the COPI, and the undisturbed anterograde progression of PC I under the conditions of COPI downregulation. The question if these potentially different type of carriers fuse with the Golgi complex independently or mutually coalesce earlier remains to be answered.

In summary, we present three different sets of data, namely colocalization, downregulation by RNAi and functional analysis under the conditions of cDNA-GFPs over-expression, which clearly indicate that the trafficking routes of ts-O45-G and PC I are different at the molecular level. The differences were observed not only at the late stage but also during the early stages of cargo progression. Taking into consideration that PC I is a natural cellular cargo, the way it is secreted might represent an essential secretory route in mammalian cells. The differences in ts-O45-G and PC I trafficking could represent specificities for various classes of cargo, like TM, soluble or large and complex

Figure 6: Examples how cDNA-GFPs over-expression change localization of secretory pathway proteins. HeLa cells were transfected with cDNA-GFPs, incubated for 24 h and fixed and immunostained for the respective sub-cellular markers (for details, see *Materials and Methods*). The GTP-restricted dominant-negative mutant of the Sar1p GTPase (SAR1p$^{[H79G]}$) exerts profound alterations on the secretory pathway. Less intense, but easily identifiable perturbations, are caused by the over-expression of the unknown protein AL136588, which has an effect only on the secretion of ts-O45-G, but not PCI, and GOT1B protein, which inhibits secretion of PC I and ts-O45-G. An uncharacterized protein AL136916 induces alterations of late, but not early secretory pathway markers, when over-expressed. Asterisks indicate transfected cells, and arrows indicate altered cells. Scale bar = 20 μm.

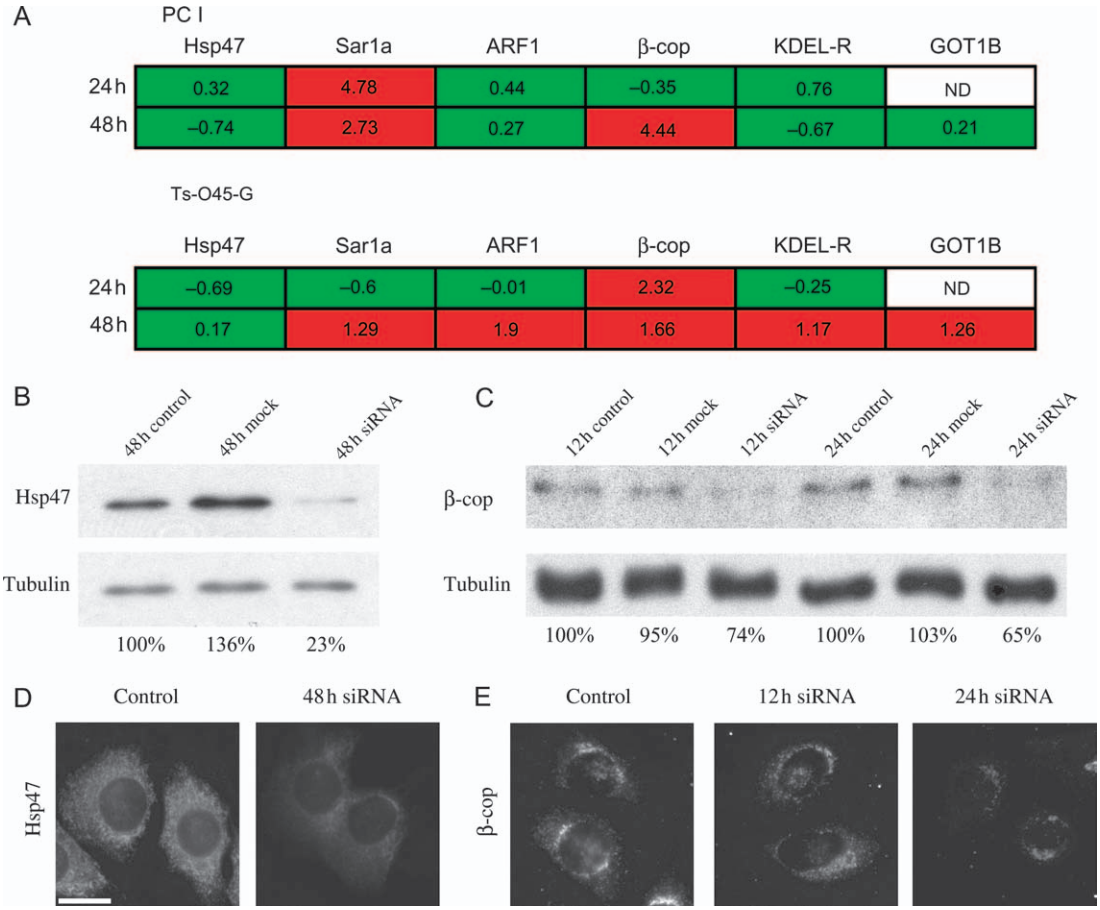

Figure 7: Secretion of PC I and ts-O45-G under the conditions of downregulation by RNAi components of the early secretory pathway. A) Secretion of PC I and ts-O45-G under the conditions of downregulation by siRNAs proteins of the early secretory pathway. The changes in secretion of both cargoes are expressed as a normalized mean difference between cells transfected with the respective siRNA and cells transfected with the control siRNA (see *Materials and Methods*). Values bigger than −1 or 1 represent statistically significant changes of secretion efficiencies and are coloured in red; values smaller than −1 or 1 represent no significant changes and are coloured in green. B and C) The efficiency of the siRNAs against Hsp47 and β-COP were confirmed by Western blot analysis. Blots for tubulin from the same cells are shown to indicate protein loadings. Numbers shows the remaining amount of Hsp47 or β-COP, normalized to the tubulin amounts. D and E) The efficiency of the siRNAs against Hsp47 and β-COP according immunofluorescence stainings. Scale bar = 20 μm. ND, not determined.

proteins. The challenge now is to refine what these differences encode and how are they occurring and maintained.

Materials and Methods

Materials

GFP-tagged open reading frames were generated and prepared as described earlier (53). Recombinant adenoviruses encoding the secretory marker protein ts-O45-G tagged with either CFP or YFP were as described (54). The mouse monoclonal anti-ts-O45-G antibody 'VG' recognising the extra-cellular epitope was a gift from K. Simons (MPI-CBG, Dresden, Germany). The mouse monoclonal anti-ERGIC53 was a gift from H. P. Hauri (Basel, Switzerland), mouse monoclonal anti-BiP and anti-PDI antibodies were a gift from S. Fuller (Oxford, UK), rabbit polyclonal EAGE for labelling β-COP (55), mouse monoclonal M3A5 for labelling β-COP (56). Following commercial primary antibodies were used: mouse monoclonal anti-TfR (Zymed, San Francisco, CA, USA), mouse monoclonal anti-GM130 (BD Bioscience, San Diego, CA, USA), rabbit polyclonal anti-PC I (Chemicon, Hampshire, UK), mouse monoclonal anti-Hsp47 (Stressgen, San Diego, CA, USA), rabbit polyclonal anti-sec23 for labelling COPII (Affinity BioReagents, Golden, CO, USA), polyclonal sheep anti-TGN46 (Serotec, Kidlington, UK), mouse monoclonal EEA1 (early endosomal antigen 1) for labelling endosomes (BD Bioscience), mouse monoclonal a-tubulin (Neomarkers, Fremont, CA, USA). Commercial secondary antibodies were as follows: anti-rabbit Alexa 568, anti-mouse Alexa 488 (Molecular Probes, Eugene, OR, USA), Cy5- or Cy3-labelled anti-mouse and anti-rabbit antibodies (AmershamBiosciences, Freiburg, Germany). Accession numbers of RNAi oligonucleotides (Qiagen, Hilden, Germany) for Hsp47 were SI01415127 and SI01415234, for β-COP were SI00956851 and SI00956858, for Sar1a were SI01410143 and SI01410150, for GOT1B was SI00814723, for ARF1 was SI00901635 and for KDEL-R was SI00233618. A non-silencing siRNA was as in (56). All chemical reagents were purchased from Sigma-Aldrich (Taufkirchen, Germany) unless mentioned separately.

Microscopy and image processing

For the quantitative data acquisition for functional analysis with cDNA-GFPs over-expressed and observation of cellular phenotypes, a widefield

microscope Zeiss Axiovert 200 (Carl Zeiss, Jena, Germany) was used with a 40× PlanNeoFluor NA 1.3 oil immersion objective. Colocalization studies were performed on a confocal microscope Zeiss LSM510 FCS (Carl Zeiss) using 63× PlanApochromat NA 1.4 oil immersion objective. Functional assays under conditions of downregulation by siRNA were performed on a widefield Scan^R system (www.olympus.com) using 20×/0.7 NA air UPlanApo objective. Count of colocalizing structures was performed in Image J. For this images were processed as follows: after subtraction of the background, images were filtered by the Gaussian Blur with the pixel radius 1. Only structures 4–60 pixel in size and having intensity at least 20% more than the surrounding were taken for colocalization. Quantitative evaluation of transport assays under conditions of cDNA-GFPs over-expression was performed in MetaMorph 4.6r5 (Molecular Devices Corp., Sunnyvale, CA, USA). For this images were processed as follows: after subtraction of the background structures of interest were determined by a threshold and total grey values in these structures were calculated in each cell individually. Quantitative evaluation of transport assays under conditions of downregulation by siRNAs was performed on Scan^R Analysis software (www.olympus.com) and essentially the same steps of image analysis were undertaken.

PC I and ts-O45-G transport assays

To work under the conditions of cDNA-GFPs over-expression, NIH 3T3 cells ATCC (CRL-1658) were grown on glass bottom culture dishes (MatTek, Ashland, MA, USA), to work under the conditions of downregulation by siRNAs, the cells were grown on eight-well LabTek chamber slides (Nalge Nunc) for 24 h before transfection. The cDNA-GFP constructs were transfected with Effectene reagent (Qiagen), siRNAs were transfected with Oligofectamine reagent (Invitrogen, Carlsbad, CA, USA) according producers recommendations.

For assaying PC I transport, cells transfected with cDNA-GFP constructs or siRNAs were incubated for appropriate time periods, and PC I secretion was induced by addition of a mixture consisting of 0.25 mM ascorbate and 1 mM ascorbate-2-phosphate. The PC I was chased in the presence of 100 μg/mL cycloheximide (Calbiochem, San Diego, CA, USA) at 37°C. At the desired time-points, cells were fixed with 3% paraformaldehyde, permeabilized with 0.1%Triton-X-100 and PC I was detected by immunostaining. For assaying ts-O45-G transport, cells transfected with cDNA-GFP constructs or siRNAs were verlaid with recombinant adenoviruses encoding ts-O45-G tagged with CFP or YFP to complement the colour of the transfected CFP- or YFP-tagged cDNA. After 45 minutes adenoviruses were washed away, and ts-O45-G was accumulated in the ER by incubating the cells at 39.5°C for further 18 h. Thereafter, cells were shifted to 32°C to release ts-O45-G from the ER in the presence of cycloheximide. At the desired time-points, cells were fixed with 3% paraformaldehyde and ts-O45-G on the cell surface was detected by immunostaining with a VG antibody recognising ts-O45-G at the PM. Cell nuclei were labelled with Hoechst 33342 diluted to a final concentration of 0.1 μg/mL. To measure the rate of ts-O45-G secretion at 37°C, the experiment was performed in above described way, except that before transferring the cell to 37°C, they were incubated for 5 minutes at 32°C, to ensure folding of ts-O45-G.

Quantification of PC I and ts-O45-G transport assays

In MetaMorph and Scan^R Analysis, the images containing stained cell nuclei were thresholded and binarized (pixels above the threshold value were set to 1, those below the threshold were set to 0) to define a mask corresponding each nucleus. Then each mask was dilated to encompass a maximum area of cell without touching the neighbouring ones. Total grey values corresponding amounts of expressed cDNA-GFP product, endogenous PC I, intracellular ts-O45-G-GFP, ts-O45-G-GFP at the PM were measured in each area.

The transport rate of ts-O45-G was expressed as a ratio of ts-O45-G at the PM to the total amount of ts-O45-G in each cell (57). If working with cDNA-GFPs over-expressed, average ts-O45-G transport ratios were obtained separately for the transfected and non-transfected cells. Finally, the effect of GFP-tagged cDNA over-expression was expressed as a normalized transport ratio of transfected to non-transfected cells (consequently, values below 1 indicate an inhibition of ts-O45-G trafficking). Transport rate of PC I was expressed as an amount of remaining PC I-specific fluorescence in each cell, averaged and calculated separately in transfected and non-transfected cells. The effect of cDNA-GFP over-expression was expressed as a normalized ratio of transfected to non-transfected cells (consequently, values above 1 indicate an inhibition of PC I trafficking). If working with siRNAs, cells transfected with the respective siRNA were compared with the cells transfected with the control siRNA. The significance of the inhibition effect for both cargoes was determined by a pooled standard error of the mean differences between the values of two populations of cells ($s_p = \sqrt{1/n_1 + 1/n_2}$; see (58) where s_p is the pooled standard deviation, n_1 the number of transfected and n_2 the number of non-transfected cells). Only those cDNA-GFPs, for which the mean difference between the values for transfected and non-transfected cells was twice bigger than the pooled standard error, were considered as significant effectors of trafficking. Each cDNA-GFP was tested at least two to three times with more than 30 transfected and more than 50 non-transfected cells evaluated per experiment. The significance of the inhibition effect of siRNAs was evaluated in analogous way. Each siRNA was tested at least five to six times with more than 5000 cells evaluated per experiments.

The efficiency of downregulation was evaluated by the Western blot. For this, cells were cultured in six-well plates, transfected with the respective siRNAs and incubated at various time-points. Cell lysates were subjected to the SDS–PAGE followed by the transfer to PVDF (polyvinylidene fluoride) membranes. Membranes were probed with the respective antibodies using α-tubulin as a loading control, and electrochemiluminenscence detection.

Strategy to identify where transport inhibition of ts-O45-G occurs

HeLa cells ATCC (CCL-2) were grown on glass bottom culture dishes (MatTek) for 24 h before transfection, and cDNA-GFP constructs were transfected with FuGene6 reagent according producers recommendations (Roche, Basel, Switzerland). Six hours later, cells were infected with the recombinant adenovirus encoding ts-O45-G-GFP as described above. In each cell, two parameters were calculated at a given time-point: (i) total intracellular ts-O45-G-GFP-specific fluorescence and (ii) ts-O45-G-specific fluorescence residing in the Golgi complex area. For this, the Golgi complex was visualized by the immunostainings with anti-GM130. The amount of ts-O45-G-GFP passing the Golgi complex was expressed as a normalized ratio between fluorescence intensities of ts-O45-G-GFP in the Golgi complex area to total intracellular intensity in each cell. This was done for the transfected and non-transfected cells separately, averaged and both ratios compared. The differences between non-transfected and transfected cells only then were considered significant, when a pooled standard error of mean difference (depicted as an effect size in Figure 5) was twice bigger than the difference between the two ratios. Positive values reflect that the fraction of ts-O45-G-GFP at the Golgi complex is higher in non-transfected cells, negative values – indicate the opposite. For each cDNA-GFP at each time-point, more than 30 cells were analysed.

Acknowledgments

We would like to thank Brigitte Joggerst for technical assistance, Darren Gilmour for comments on the manuscript and Holger Erfle for the help with the MetaMorph. We thank the ALMF (advanced light microscopy facility) team at European Molecular Biology Laboratory for their support with imaging and Carl Zeiss, Germany, for instrument support of the ALMF. This work has been supported by a BMBF (Bundesministerium fur Bildung und Forschung) grant FKZ01GR0423 and the Landes-stiftung Baden-Württemberg to R. P.

References

1. Lee M, Miller E, Goldberg J, Orci L, Schekman R. Bi-directional protein transport between the ER and Golgi. Annu Rev Cell Dev Biol 2004; 20:87–123.
2. Gaynor EC, Emr SD. COPI-independent anterograde transport: cargo-selective ER to Golgi protein transport in yeast COPI mutants. J Cell Biol 1997;136:789–802.
3. Muniz M, Morsomme P, Riezman H. Protein sorting upon exit from the endoplasmic reticulum. Cell 2001;104:313–320.
4. Yoo JS, Moyer BD, Bannykh S, Yoo HM, Riordan JR, Balch WE. Non-conventional trafficking of the cystic fibrosis transmembrane conductance regulator through the early secretory pathway. J Biol Chem 2002;277:11401–11409.
5. Dascher C, Balch WE. Dominant inhibitory mutants of ARF1 block endoplasmic reticulum to Golgi transport and trigger disassembly of the Golgi apparatus. J Biol Chem 1994;269:1437–1448.
6. Plutner H, Cox AD, Pind S, Khosravi-Far R, Bourne JR, Schwaninger R, Der CJ, Balch WE. Rab1b regulates vesicular transport between the endoplasmic reticulum and successive Golgi compartments. J Cell Biol 1991;115:31–43.
7. Rowe T, Dascher C, Bannykh S, Plutner H, Balch WE. Role of vesicle-associated syntaxin 5 in the assembly of pre-Golgi intermediates. Science 1998;279:696–700.
8. Hasdemir B, Fitzgerald DJ, Prior IA, Tepikin AV, Burgoyne RD. Traffic of Kv4 K+ channels mediated by KChIP1 is via a novel post-ER vesicular pathway. J Cell Biol 2005;171:459–469.
9. Lamande SR, Bateman JF. Procollagen folding and assembly: the role of endoplasmic reticulum enzymes and molecular chaperones. Semin Cell Dev Biol 1999;10:455–464.
10. Zeuschner D, Geerts WJ, van Donselaar E, Humbel BM, Slot JW, Koster AJ, Klumperman J. Immuno-electron tomography of ER exit sites reveals the existence of free COPII-coated transport carriers. Nat Cell Biol 2006;8:377–383.
11. Kaiser CA, Schekman R. Distinct sets of SEC genes govern transport vesicle formation and fusion early in the secretory pathway. Cell 1990;61:723–733.
12. Stephens DJ, Pepperkok R. Imaging of procollagen transport reveals COPI-dependent cargo sorting during ER-to-Golgi transport in mammalian cells. J Cell Sci 2002;115:1149–1160.
13. Mironov AA, Mironov AA Jr, Beznoussenko GV, Trucco A, Lupetti P, Smith JD, Geerts WJ, Koster AJ, Burger KN, Martone ME, Deerinck TJ, Ellisman MH, Luini A. ER-to-Golgi carriers arise through direct en bloc protrusion and multistage maturation of specialized ER exit domains. Dev Cell 2003;4:584–595.
14. Aridor M, Bannykh SI, Rowe T, Balch WE. Sequential coupling between COPII and COPI vesicle coats in endoplasmic reticulum to Golgi transport. J Cell Biol 1995;131:875–893.
15. Stephens DJ, Pepperkok R. Differential effects of a GTP-restricted mutant of Sar1p on segregation of cargo during export from the endoplasmic reticulum. J Cell Sci 2004;117:3635–3644.
16. Starkuviene V, Liebel U, Simpson JC, Erfle H, Poustka A, Wiemann S, Pepperkok R. High-content screening microscopy identifies novel proteins with a putative role in secretory membrane traffic. Genome Res 2004;14:1948–1956.
17. Leblond CP. Synthesis and secretion of collagen by cells of connective tissue, bone, and dentin. Anat Rec 1989;224:123–138.
18. Cho MI, Garant PR. Sequential events in the formation of collagen secretion granules with special reference to the development of segment-long-spacing-like aggregates. Anat Rec 1981;199:309–320.
19. Walmsley AR, Batten MR, Lad U, Bulleid NJ. Intracellular retention of procollagen within the endoplasmic reticulum is mediated by prolyl 4-hydroxylase. J Biol Chem 1999;274:14884–14892.
20. Bienkowski RS, Baum BJ, Crystal RG. Fibroblasts degrade newly synthesised collagen within the cell before secretion. Nature 1978;276:413–416.
21. Ripley CR, Bienkowski RS. Localization of procollagen I in the lysosome/endosome system of human fibroblasts. Exp Cell Res 1997;236: 147–154.
22. Sutherland R, Delia D, Schneider C, Newman R, Kemshead J, Greaves M. Ubiquitous cell-surface glycoprotein on tumor cells is proliferation-associated receptor for transferrin. PNAS 1981;78: 4515–4519.
23. Fukuda M, Viitala J, Matteson J, Carlsson SR. Cloning of cDNAs encoding human lysosomal membrane glycoproteins, h-lamp-1 and h-lamp-2. Comparison of their deduced amino acid sequences. J Biol Chem 1988;263:18920–18928.
24. Hirschberg K, Miller CM, Ellenberg J, Presley JF, Siggia ED, Phair RD, Lippincott-Schwartz J. Kinetic analysis of secretory protein traffic and characterization of golgi to plasma membrane transport intermediates in living cells. J Cell Biol 1998;143:1485–1503.
25. Pepperkok R, Lowe M, Burke B, Kreis TE. Three distinct steps in transport of vesicular stomatitis virus glycoprotein from the ER to the cell surface in vivo with differential sensitivities to GTP gamma S. J Cell Sci 1998;111:1877–1888.
26. Presley JF, Cole NB, Schroer TA, Hirschberg K, Zaal KJ, Lippincott-Schwartz J. ER-to-Golgi transport visualized in living cells. Nature 1997; 389:81–85.
27. Kreis TE, Lodish HF. Oligomerization is essential for transport of vesicular stomatitis viral glycoprotein to the cell surface. Cell 1986;46: 929–937.
28. Zilberstein A, Snider MD, Porter M, Lodish HF. Mutants of vesicular stomatitis virus blocked at different stages in maturation of the viral glycoprotein. Cell 1980;21:417–421.
29. Bonifacino JS, Traub LM. Signals for sorting of transmembrane proteins to endosomes and lysosomes. Annu Rev Biochem 2003; 72:395–447.
30. Scales SJ, Pepperkok R, Kreis TE. Visualization of ER-to-Golgi transport in living cells reveals a sequential mode of action for COPII and COPI. Cell 1997;90:1137–1148.
31. Griffiths G, Pepperkok R, Locker JK, Kreis TE. Immunocytochemical localization of beta-COP to the ER-Golgi boundary and the TGN. J Cell Sci 1995;108:2839–2856.
32. Hosokawa N, Nagata K. Procollagen binds to both prolyl 4-hydroxylase/protein disulfide isomerase and HSP47 within the endoplasmic reticulum in the absence of ascorbate. FEBS Lett 2000;466: 19–25.
33. Satoh M, Hirayoshi K, Yokota S, Hosokawa N, Nagata K. Intracellular interaction of collagen-specific stress protein HSP47 with newly synthesized procollagen. J Cell Biol 1996;133:469–483.
34. Koide T, Asada S, Takahara Y, Nishikawa Y, Nagata K, Kitagawa K. Specific recognition of the collagen triple helix by chaperone HSP47: minimal structural requirement and spatial molecular orientation. J Biol Chem 2006;281:3432–3438.
35. Smith T, Ferreira LR, Hebert C, Norris K, Sauk JJ. Hsp47 and cyclophilin B traverse the endoplasmic reticulum with procollagen into pre-Golgi intermediate vesicles. A role for Hsp47 and cyclophilin B in the export of procollagen from the endoplasmic reticulum. J Biol Chem 1995;270: 18323–18328.
36. Nagata K. HSP47 as a collagen-specific molecular chaperone: function and expression in normal mouse development. Semin Cell Dev Biol 2003;14:275–282.
37. Bruckner P, Eikenberry EF. Formation of the triple helix of type I procollagen in cellulo. Temperature-dependent kinetics support a model based on cis in equilibrium trans isomerization of peptide bonds. Eur J Biochem 1984;140:391–395.

38. Dilcher M, Veith B, Chidambaram S, Hartmann E, Schmitt HD, Fischer von Mollard G. Use1p is a yeast SNARE protein required for retrograde traffic to the ER. EMBO J 2003;22:3664–3674.
39. Wang H, Zhang Q, Zhu D. hSGT interacts with the N-terminal region of myostatin. Biochem Biophys Res Commun 2003;311:877–883.
40. Neubrand VE, Will RD, Mobius W, Poustka A, Wiemann S, Schu P, Dotti CG, Pepperkok R, Simpson JC. Gamma-BAR, a novel AP-1-interacting protein involved in post-Golgi trafficking. EMBO J 2005;24: 1122–1133.
41. Liu FH, Wu SJ, Hu SM, Hsiao CD, Wang C. Specific interaction of the 70-kDa heat shock cognate protein with the tetratricopeptide repeats. J Biol Chem 1999;274:34425–34432.
42. Toomre D, Keller P, White J, Olivo JC, Simons K. Dual-color visualization of trans-Golgi network to plasma membrane traffic along microtubules in living cells. J Cell Sci 1999;112:21–33.
43. Shima DT, Scales SJ, Kreis TE, Pepperkok R. Segregation of COPI-rich and anterograde-cargo-rich domains in endoplasmic-reticulum-to-Golgi transport complexes. Curr Biol 1997;9:821–824.
44. Conchon S, Cao X, Barlowe C, Pelham HR. Got1p and Sft2p: membrane proteins involved in traffic to the Golgi complex. EMBO J 1999; 15:3934–3946.
45. Mironov AA, Beznoussenko GV, Nicoziani P, Martella O, Trucco A, Kweon HS, Di Giandomenico D, Polishchuk RS, Fusella A, Lupetti P, Berger EG, Geerts WJ, Koster AJ, Burger KN, Luini A. Small cargo proteins and large aggregates can traverse the Golgi by a common mechanism without leaving the lumen of cisternae. J Cell Biol 2001; 155:1225–1238.
46. Page LJ, Sowerby PJ, Lui WW, Robinson MS. Gamma-synergin: an EH domain-containing protein that interacts with gamma-adaptin. J Cell Biol 1999;6:993–1004.
47. Polishchuk EV, Di Pentima A, Luini A, Polishchuk RS. Mechanism of constitutive export from the golgi: bulk flow via the formation, protrusion, and en bloc cleavage of large trans-golgi network tubular domains. Mol Biol Cell 2003;14:4470–4485.
48. Bonazzi M, Spano S, Turacchio G, Cericola C, Valente C, Colanzi A, Kweon HS, Hsu VW, Polishchuck EV, Polishchuck RS, Sallese M, Pulvirenti T, Corda D, Luini A. CtBP3/BARS drives membrane fission in dynamin-independent transport pathways. Nat Cell Biol 2005;7: 570–580.
49. Ishida Y, Kubota H, Yamamoto A, Kitamura A, Bachinger HP, Nagata K. Type I collagen in Hsp47-null cells is aggregated in endoplasmic reticulum and deficient in N-propeptide processing and fibrillogenesis. Mol Cell Biol 2006;17:2346–2355.
50. Aoe T, Huber I, Vasudevan C, Watkins SC, Romero G, Cassel D, Hsu VW. The KDEL receptor regulates a GTPase-activating protein for ADP-ribosylation factor 1 by interacting with its non-catalytic domain. J Biol Chem 1999;274:20454–20459.
51. Lang MR, Lapierre LA, Frotscher M, Goldenring JR, Knapik EW. Secretory COPII coat component Sec23a is essential for craniofacial chondrocyte maturation. Nat Genet 2006;38:1198–1203.
52. Boyadjiev SA, Fromme JC, Ben J, Chong SS, Nauta C, Hur DJ, Zhang G, Hammamoto S, Schekman R, Ravazzola M, Orci L, Eyaid W. Cranio-lenticulo-sutural dysplasia is caused by a SEC23A mutation leading to abnormal endoplasmic-reticulum-to-Golgi trafficking. Nat Genet 2006;38:1192–1197.
53. Simpson JC, Wellenreuther R, Poustka A, Pepperkok R, Wiemann S. Systematic subcellular localization of novel proteins identified by large-scale cDNA sequencing. EMBO Rep 2000;1:287–292.
54. Keller P, Toomre D, Diaz E, White J, Simons K. Multicolour imaging of post-Golgi sorting and trafficking in live cells. Nat Cell Biol 2001;3: 140–149.
55. Pepperkok R, Scheel J, Horstmann H, Hauri HP, Griffiths G, Kreis TE. Beta-COP is essential for biosynthetic membrane transport from the endoplasmic reticulum to the Golgi complex in vivo. Cell 1993;74: 71–82.
56. Allan VJ, Kreis T. A microtubule-binding protein associated with membranes of the Golgi Apparatus. J Cell Biol 1986;103:2229–2239.
57. Liebel U, Starkuviene V, Erfle H, Simpson JC, Poustka A, Wiemann S, Pepperkok R. A microscope-based screening platform for large-scale functional protein analysis in intact cells. FEBS Lett 2003;20:394–398.
58. Hassard TH. Understanding biostatistics. Mosby-Year Book, 1991, 156–157.
59. Heaton JH, Dlakic WM, Dlakic M, Gelehrter TD. Identification and cDNA cloning of a novel RNA-binding protein that interacts with the cyclic nucleotide-responsive sequence in the type-1 plasminogen activator inhibitor mRNA. J Biol Chem 2001;276:3341–3347.
60. Frank CG, Aebi M. ALG9 mannosyltransferase is involved in two different steps of lipid-linked oligosaccharide biosynthesis. Glycobiology 2005;15:1156–1163.
61. Dusetti NJ, Jiang Y, Vaccaro MI, Tomasini R, Azizi Samir A, Calvo EL, Ropolo A, Fiedler F, Mallo GV, Dagorn JC, Iovanna JL. Cloning and expression of the rat vacuole membrane protein 1 (VMP1), a new gene activated in pancreas with acute pancreatitis, which promotes vacuole formation. Biochem Biophys Res Commun 2002;290:641–649.
62. Calero M, Winand NJ, Collins RN. Identification of the novel proteins Yip4p and Yip5p as Rab GTPase interacting factors. FEBS Lett 2002;515:89–98.
63. Modregger J, Ritter B, Witter B, Paulsson M, Plomann M. All three PACSIN isoforms bind to endocytic proteins and inhibit endocytosis. J Cell Sci 2000;113:4511–4521.